APPLIED SCIENCES AND ENGINEERING

Deciphering neutrophil dynamics: Enhanced phagocytosis of elastic particles and impact on vascular-targeted carrier performance

Jonathan K. Lee[1]†, M.Valentina Guevara[1]†, Oluwaseun D. Akanbi[1], J. Damon Hoff[2], Daniel Kupor[1], Emma R. Brannon[1], Omolola Eniola-Adefeso[1]*

Particle elasticity has widely been established to substantially influence immune cell clearance and circulation time of vascular-targeted carriers (VTCs). However, prior studies have primarily investigated interactions with macrophages, monocytic cell lines, and in vivo murine models. Interactions between particles and human neutrophils remain largely unexplored, although they represent a critical aspect of VTC performance. Here, we explore the impact of particle elasticity on primary human neutrophil phagocytosis using polyethylene glycol–based particles of different elastic moduli. We found that neutrophils effectively phagocytose deformable particles irrespective of their modulus, indicating a departure from established phagocytosis trends seen with other types of immune cells. These findings highlight the observed phenotypic difference between different types of phagocytes and underscore the need to characterize VTC performance using various cell types and animal models that represent human systems closely.

INTRODUCTION

Vascular-targeted carriers (VTCs) are a promising drug delivery approach for treating various conditions, including cancer and coronary artery disease (*1*, *2*). However, a notable issue that limits VTCs' in vivo efficacy is their rapid removal from circulation through filtration via reticuloendothelial system (RES) organs and clearance by phagocytic leukocytes (*3*–*5*). Over the years, researchers have explored ways to design VTCs to avoid phagocytic uptake and achieve longer circulation times. Most of these efforts have focused on non-fouling surface coatings such as polyethylene glycol (PEG), cell membrane–derived coatings, and zwitterionic coatings (*6*–*8*). Particle elasticity emerged as an important factor in designing particles for intravenous drug delivery applications in recent years due to the favorable effects of a softer particle on reducing phagocytosis by immune cells such as macrophages and monocytes (*9*, *10*).

Softer particles have been shown to have a lower tendency to be phagocytosed by macrophages and monocytes (*10*, *11*), suggesting that they would be more effective for drug delivery. For instance, a study involving PEG-based nanoparticles showed that soft (0.255 kPa) and hard nanoparticles (3000 kPa) have significant differences in cellular uptake by J774 macrophages, where the stiff particles were taken up at a greater rate than their softer counterpart (*9*). Similarly, polyacrylamide microparticles exposed to mouse bone marrow–derived macrophages confirmed that softer particles, reported as three times softer than rigid counterparts, are less likely to be internalized by these phagocytes (*12*). In vivo mouse assays also suggest that particle elasticity is an important factor in extending circulation time, where soft nanoparticles were shown to have a longer circulation time and a higher likelihood of successful delivery to target sites due to their ability to avoid both phagocytosis and filtration by RES organs (*9*, *13*–*15*). However, most work evaluating particle deformability as a viable approach to minimize or avoid drug carrier phagocytosis has been in vitro with macrophages and monocytic cell lines. In addition, in vivo experiments in animal models, primarily murine, may not fully represent phagocytic phenotypes in a human system.

Neutrophils are highly efficient phagocytes that comprise 50 to 70% of all immune cells circulating in human blood, with monocytes and lymphocytes at 25 to 33% and <10%, respectively (*16*). VTCs are designed to be delivered intravenously into the human body to target diseases via the vascular wall; thus, neutrophils are the primary phagocytes with which VTCs will encounter first. However, little is known about how neutrophils interact with soft particles and whether the relationship between particle elasticity and phagocytosis holds in primary human cells. Previous studies have shown neutrophils may not behave the same way as typically studied phagocytes. For instance, one notable study found that neutrophils more readily phagocytosed PEGylated polystyrene (PS) particles than non-PEGylated particles in the presence of human plasma, a departure from trends seen in macrophages where PEGylation typically acts as a stealth coating (*17*). Another study found that neutrophils unexpectedly phagocytosed rods at a significantly greater rate than spherical particles, while macrophages exhibited lower phagocytosis of rod-shaped particles as expected (*18*).

In this work, we investigate the effects of particle elasticity on neutrophil phagocytosis. We exposed deformable hydrogel particles of 2-μm and 500-nm sizes with varying Young's modulus to human neutrophils in whole blood and quantified particle phagocytosis via flow cytometry. The 2-μm particles are explored on the basis of previous literature, demonstrating that they are the most efficient at concentrating at the vascular wall for vascular targeting, colocalizing with neutrophils in the bloodstream (*19*–*22*). In addition, Fish *et al.* (*1*) found that more nanoparticles (50-nm PS) reach the vascular wall in vivo in mice when loaded inside deformable 2-μm PEG hydrogel spheres than same-sized nanoparticles freely injected into the bloodstream. The 500-nm spheres are within the size range others have explored for various in vivo applications and can be adequately visualized with fluorescent imaging and flow cytometry. Additional hydrogel materials were also investigated to determine the potential interplay between particle surface chemistry and particle elasticity.

[1]Department of Chemical Engineering, University of Michigan, Ann Arbor, MI 48109, USA. [2]Small Molecule Analysis Group, Department of Chemistry, University of Michigan, Ann Arbor, MI 48109, USA.
*Corresponding author. Email: lolaa@umich.edu
†These authors contributed equally to this work.

Further understanding of interactions between particles and neutrophils will be invaluable in optimizing carrier design in vascular-targeted delivery.

RESULTS

Evaluation of neutrophil phagocytosis of PEG particles of various elasticities

We evaluated the uptake of 2-μm and 500-nm deformable PEG-based hydrogel particles by primary human neutrophils in whole blood relative to the uptake of rigid PS particles. Fluorescent 2-μm and 500-nm PS particles were purchased from Polysciences, and deformable PEG particles with embedded rhodamine dye were fabricated in-house, as previously described (*23*). The moduli for the 2-μm and 500-nm PEG particles fabricated with 15, 20, 40, and 50% PEG weight were ~23, ~113, ~300, and ~500 kPa, respectively (*23*). The modulus of PS has been reported to be in the range of 2 to 8 GPa, over three orders of magnitude greater than our stiffest hydrogel formulation (*24*). Table S1 shows the characterization of PS and PEG particles used for our phagocytosis assay, including size and particle charge.

Particles were incubated in human blood for 2 hours with concentrations resulting in ~2 and 20 particles per neutrophils for 2-μm and 500-nm particles, respectively, and the cell-particle association was evaluated via flow cytometry, using double-positive stains for CD11b and CD45 to identify immune cells in whole blood. The neutrophil population was then determined using forward and side scatter, as described previously (*17*, *18*). Particle-positive cells were identified by either a positive signal for fluorescein for PS or rhodamine for PEG. A schematic of the flow cytometry analysis is shown in fig. S1.

Figure 1A reports human neutrophil uptake of 500-nm PS and PEG particles in whole blood. We observed a 1.7-, 1.3-, 1.6-, and 1.9-fold increase in 500-nm PEG hydrogel uptake compared to that in 500-nm PS for the 50, 40, 20, and 15% PEG, respectively. Despite the slight increase in the percentage of PEG particle–positive neutrophils, we did

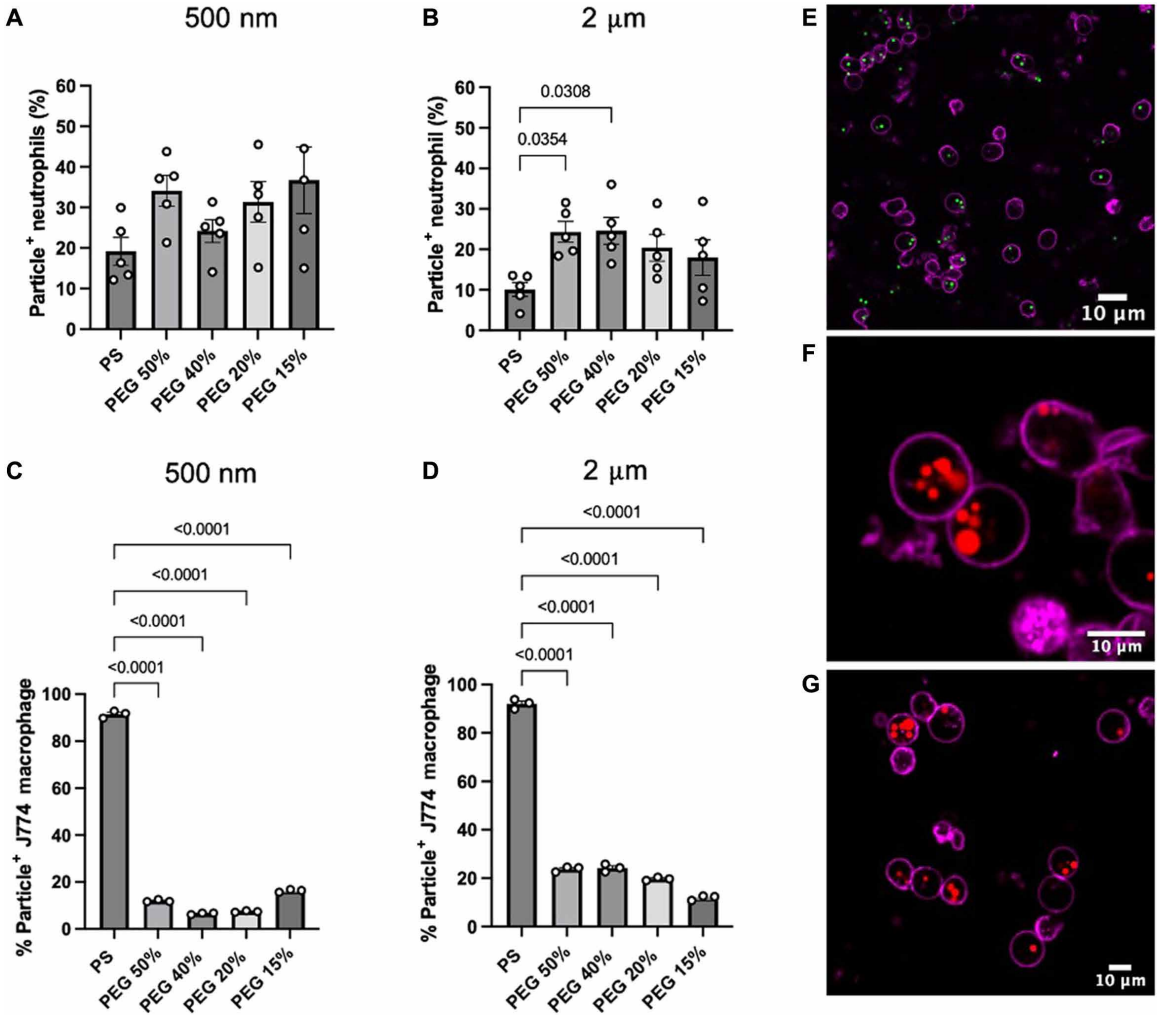

Fig. 1. Phagocytosis of 2-μm- and 500-nm-sized PS and PEG particles. Percentage of particle-positive cells by (**A** and **B**) primary human neutrophils in whole blood and (**C** and **D**) J774 macrophages in Dulbecco's modified Eagle's medium (DMEM) with 10% fetal bovine serum (FBS). Samples were incubated with cells for 2 hours before staining, fixing, and analyzing with flow cytometry. At least 5000 events were recorded for each assay. Confocal microscopy images of isolated human neutrophils confirmed that (**E**) 2-μm PS, (**F**) 2-μm 50% PEG, (**G**) and 2-μm 15% PEG particles were internalized by the cells. Statistical analysis was performed using one-way ANOVA with Tukey's multiple comparisons posttest. For (A) and (B), graph bars show the average particle-positive neutrophils with SEM. Each circle represents an individual blood donor. For (C) and (D), graph bars show the average of three technical replicates of J774 macrophage uptake. For (E) to (G), the scale bar is 10 μm.

not observe statistical differences in the percentage of particle-positive cells that phagocytosed 500-nm PEG–based hydrogels and PS particles. Likewise, we found that the different types of 500-nm PEG hydrogels exhibited similar particle-association levels. Thus, no statistical differences in particle uptake were observed between the various particle elasticities. Overall, we found that human neutrophils associated with 500-nm PEG hydrogels of various elasticities and PS particles to a similar extent despite the wide range of Young's moduli they encompassed (25 kPa to 8 GPa), contradicting previous reports for phagocytic assays macrophages and other monocytic cells (*9*, *11*, *25*).

Figure 1B depicts phagocytosis of 2-μm PEG and PS particles by human neutrophils. We found that all 2-μm PEG hydrogels of varying elasticities were taken up by neutrophils nearly twice as much as the 2-μm PS group. Specifically, we observed a 2.5-fold increase in the percentage of particle-positive neutrophils for the 50 and 40% PEG hydrogels compared to that for 2-μm PS particles. Similar to the 500-nm PEG hydrogels, we found no statistical differences in the percentage of particle internalization among the different types of 2-μm PEG hydrogels used in this study.

Besides quantifying the percentage of particle-positive neutrophils, we extended our analysis to determine the extent of particle uptake per neutrophil. Using our flow cytometry analysis, we quantified the particle-positive populations' median fluorescence intensity (MFI). We then normalized these values to the MFI of each particle type to obtain an approximate number of particles per cell. We found more PEG hydrogels internalized per neutrophil compared to PS particles. We observed no differences in the extent of uptake between the different types of 2-μm PEG hydrogels or between the several 500-nm PEG hydrogels (fig. S2). We confirmed these results using confocal microscopy, where we found that 2-μm PS particles (green) and 2-μm 50 and 15% PEG hydrogels (red) were readily localized in the interior of the neutrophil cell membrane (purple). We observed that most neutrophils internalized multiple 2-μm PEG hydrogels, while neutrophils incubated with 2-μm PS carried fewer particles per cell (Fig. 1, E to G). We measured the zeta potential of the different types of PEG hydrogels and PS particles to determine whether particle internalization of PEG hydrogels was due to particle surface charge. As reported in table S1, both PS particles and all PEG-based hydrogels were negatively charged. Hence, the observed differences in particle targeting per cell are likely not due to particle surface charge.

We repeated our uptake assays using J774 macrophages, the most common cell line used in phagocytosis assays (Fig. 1, C and D). As shown in Fig. 1C, the 50, 40, 20, and 15% 500-nm PEG spheres had an 8-, 14-, 12-, and a 6-fold decrease in uptake, respectively, compared to their stiff PS counterpart. A similar trend was found for 2-μm particle uptake by J774 macrophages, where 50, 40, 20, and 15% PEG hydrogels had a four-, four-, five-, and eightfold decrease in uptake compared to the 2-μm PS, respectively (Fig. 1D). The uptake of 2-μm PEG hydrogels by J774 macrophages resulted in a downward trend of phagocytosis levels with decreasing particle modulus, matching prior works with this cell line with respect to particle elasticity (*2*, *9*, *26*).

In summary, we observed that primary human neutrophils could rapidly phagocytose a range of deformable 2-μm and 500-nm PEG hydrogels to a similar or higher extent as rigid PS particles. Similar observations were made with mouse neutrophils, where mouse neutrophils phagocytosed 2-μm PEG particles and PS particles at comparable levels (fig. S3). Our results also showed that other phagocytic cells, such as macrophages, cannot readily internalize our deformable PEG particles as they do rigid PS particles.

Evaluation of the impact of particle chemistry on neutrophil phagocytosis of deformable particles

To determine whether the differences in phagocytosis of deformable particles between neutrophils and macrophages reported in Fig. 1 are due to particle deformability and not changes in surface chemistry between PS and PEG, we next sought to fabricate hydrogel particles of a different material from PEG. For this purpose, we used hyaluronic acid methacrylate (HAMA) as a PEG-analogous deformable material. Hyaluronic acid (HA) is a gel-like extracellular matrix component, and recent studies have used chemically modified HA for numerous applications, including cell scaffolding and pulmonary and vascular delivery (*27*–*32*). First, we characterized the elasticity of 10, 8, and 5% HA-based hydrogel material using bulk hydrogel rheometry to determine Young's modulus. A shear modulus was first measured, and Young's modulus was calculated using a Poisson's ratio of 0.5 for an elastic material, such as swollen or hydrated hydrogels (*33*). As shown in Fig. 2A, Young's modulus for

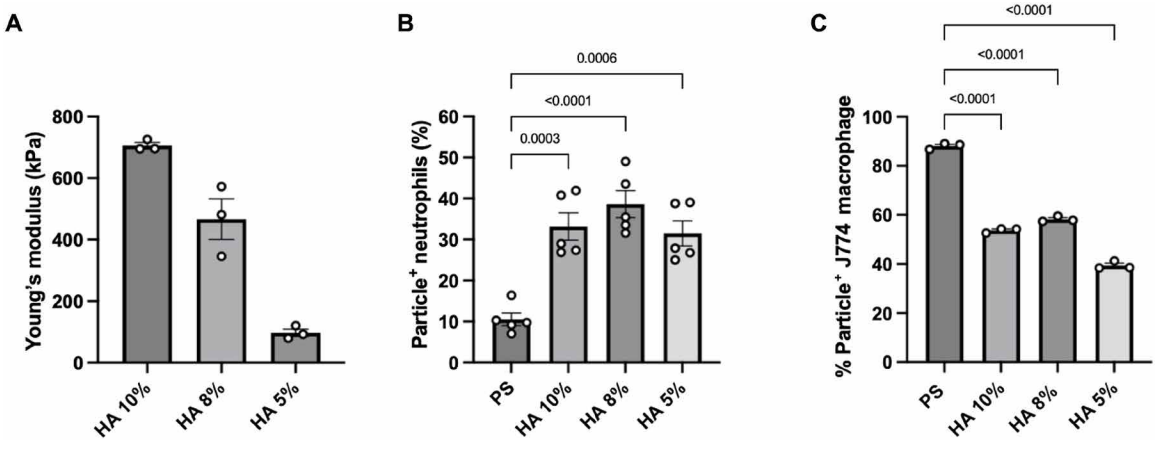

Fig. 2. Rheometry and uptake of HA-based hydrogels. (**A**) Rheometry of bulk HA hydrogel samples, indicating a wide range of Young's moduli. Uptake of 2-μm-sized HA-derived spherical particles by (**B**) primary human neutrophils in whole blood and (**C**) J774 macrophages in DMEM and 10% FBS medium. Statistics for the phagocytosis assays were performed using one-way analysis of variance (ANOVA) with Tukey's multiple comparisons test. Bars represent the average percentage of particle-positive cells, and error bars represent SEM with $n = 5$ blood donors for neutrophils and $n = 3$ technical replicates for J774 macrophages and rheometry samples.

the bulk hydrogel was determined to be 705.6, 466.2, and 97.2 kPa for the 10, 8, and 5% HA hydrogels, respectively.

We fabricated 2-μm spherical hydrogels of 5, 8, and 10% weight HA (fig. S4) and repeated our uptake assays with human neutrophils in whole blood and with J774 macrophages. The 2-μm hydrogel size was chosen because we observed a statistical increase in particle association with neutrophils when incubated with 2-μm 50 and 40% PEG hydrogels compared to 2-μm PS.

Figure 2B shows that human neutrophils phagocytosed the different types of 2-μm HA-based hydrogels at nearly equal levels regardless of the HA particle modulus. Likewise, we observed a significant 3-, 3.6-, and 2.9-fold increase in neutrophil-particle association compared to that in 2-μm PS for HA hydrogels of 10, 8, and 5%, respectively. Conversely, when HA-based hydrogels were incubated with J774 macrophages at a particle-to-cell ratio of 40, we observed a significant decrease in the uptake of HA particles, as seen with PEG hydrogels (Fig. 2C). The uptake of 10, 8, and 5% HA particles was significantly 1.6-, 1.5-, and 2.2-fold lower than the 2-μm PS control, respectively.

Generally, we found that human neutrophils are associated with 2-μm HA hydrogels of various elasticities to a similar extent, and a more significant percentage of neutrophils phagocytosed HA-based hydrogels compared to that of PS as seen with the 2-μm PEG hydrogels. Consistent with the literature and our PEG hydrogel uptake study, our results also showed that J774 macrophages have reduced uptake of deformable HA-hydrogels compared to the rigid PS spheres. We observed that macrophages internalized more HA hydrogels compared to PEG particles despite having similar Young's moduli (Figs. 1 and 2). Nevertheless, we found that neutrophils can phagocytose a wide range of particles with different elasticities and particle chemistry, while other phagocytes might still be limited to particle deformability and composition.

Visual observation of deformable PEG particles phagocytosis in optical tweezer assays

While the phagocytosis assays performed using particles in whole blood allow for analysis of neutrophil behavior on a population level, we were interested in visualizing cell-particle interactions in real time to observe the behavior of single cells and any apparent effects of membrane wrapping on deformable particles. To achieve this, we used an optical tweezer system previously used in similar studies for imaging the engulfment of PS particles by neutrophils (*34*, *35*). Microspheres and leukocytes were incubated in the presence of an optical tweezer, allowing for single-particle manipulation. As shown in Fig. 3, when a 2-μm PS particle was in contact with a neutrophil, the neutrophil captured the particle on its membrane surface. It begins engulfing the particle during the 5-min window in which the cell was observed, and, by the 2-min mark, the PS particle is fully engulfed by the cell. Similarly, when a 2-μm 50% PEG hydrogel was delivered to a neutrophil, it was visually fully inside the cell by the 3-min mark. These observations are consistent with the previous phagocytosis assays in Fig. 1, where we confirmed via flow cytometry and confocal microscopy the internalization of PS and PEG particles by human neutrophils.

When J774 macrophages were used instead of neutrophils, we observed differences in the particle-cell interactions. As shown in Fig. 3, a macrophage was observed to engulf a 2-μm PS particle within 2 min, similar to the timescale for phagocytosis of a particle by a neutrophil. However, when a PEG particle was in contact with a macrophage, the particle was not fully engulfed by the cell, even by the 5-min mark. The particle instead stayed on the periphery of the cell membrane. When the optical tweezers were moved off the particle after the assay, the particle detached from the cell, indicating the particle was only weakly bound to the cell membrane.

As expected, when both neutrophils and J774 macrophages were brought into contact with a PS particle, the apparent shape of the particle remained unchanged throughout the engulfment process due to the rigidity of PS. However, we were still unable to detect any shape change when the cells engaged 50% PEG hydrogel particles, despite the particle modulus being well below the stiffness of other particle types shown to deform when engulfed by macrophages (*36*, *37*).

Evaluation of effects of zeta potential on neutrophil phagocytosis of PEG hydrogels

Particle surface charge, as defined by the zeta potential, has been shown to affect phagocytosis in macrophages (*38*, *39*). Thus, we investigated the potential interplay between particle zeta potential and deformability and phagocytosis by neutrophils. To alter the zeta potential, we adjusted the PEG polymer formulation to include an amino-containing linker, 2-aminoethyl methacrylate hydrochloride (AEM), in place of 2-carboxyethyl acrylate (CEA), resulting in positively charged particles. We used a mixture of AEM and CEA to achieve near-neutrally charged particles, i.e., a zeta potential as close to zero. We confirmed that the zeta potential was altered from the negative charge typically associated with incorporating the carboxylic acid–containing CEA and that a combination of CEA and AEM resulted in a roughly neutrally charged PEG particle, as shown in fig. S5. Tables S1 and S2 show the zeta potential characterization of the 2-μm PEG particles used for this assay.

We saw comparable uptake levels across all zeta potentials when 2-μm 50% PEG particles of various surface charges were incubated with neutrophils in whole blood (Fig. 4A). For the 2-μm 15% PEG hydrogels, negatively and neutrally charged particles exhibited nearly the same uptake levels. However, the uptake of the amino-coated 15% PEG particles was 1.5- and 1.7-fold greater than the carboxy-coated and neutral 15% particles, respectively (Fig. 4B).

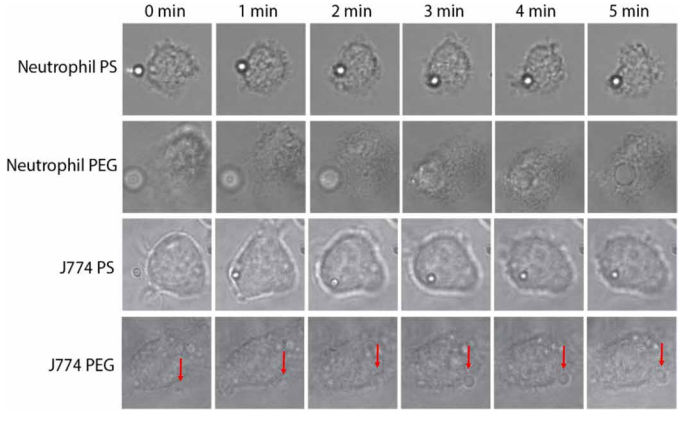

Fig. 3. Optical tweezer images where a single 2-μm particle was brought into contact with a cell. Assays were carried out with either primary human neutrophils with PS/PEG or cultured J774 macrophages with PS/PEG. Frames were selected at 1-min intervals to visualize particles as they were engulfed by cells. The PEG particle was unable to be phagocytosed by the J774 macrophage, as indicated by the red arrow near the periphery of the cell.

Next, we conducted phagocytosis assays with isolated neutrophils in RPMI medium to see whether the cells would differentially phagocytose particles of different surface charges in the absence of plasma proteins because zeta potential strongly affects the adsorption of opsonins that drive phagocytosis (*40*–*42*). As shown in fig. S6, we saw similar uptake levels for the 2-μm 15 and 50% PEG particles across all zeta potentials tested. However, the relative uptake of particles in medium was notably lower than in whole blood, likely from the absence of opsonins that typically drive phagocytosis, such as immunoglobulins and apolipoproteins (*13*, *43*, *44*).

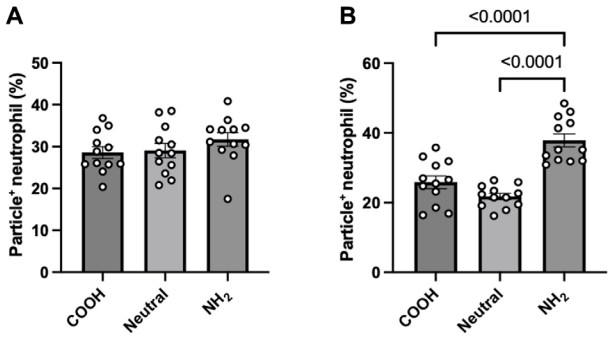

Fig. 4. Uptake of 2-μm PEG particles with varying zeta potential. The 2-μm-sized (**A**) 50% PEG and (**B**) 15% PEG particles of varying zeta potentials (either positive, negative, or neutral) were incubated with primary human neutrophils in whole blood. Displayed zeta potentials confirmed successful surface modification of surface charge using an amino-group–containing linker. Significance was determined using one-way ANOVA with Tukey's multiple comparisons test. Error bars represent SEM where $n = 12$ independent blood donors.

Evaluation of particle surface functionalization impact on particle neutrophil phagocytosis in whole blood

Particle surface functionalization with targeting ligands is particularly relevant for those used as VTCs. Because micron-sized VTCs are most effective at co-localizing with neutrophils in blood flow, i.e., in the red blood cell (RBC)–free layer of the vascular lumen (*45*), we next used functionalized particles to elucidate any impacts of particle surface conjugation on neutrophil phagocytosis of our 2-μm PEG particles. We used 1-Ethyl-3-[3-dimethylaminopropyl]carbodiimide hydrochloride (EDC) coupling chemistry to activate carboxylic acid groups on the PEG particle surface before linking the protein avidin, commonly used as a linker for conjugating additional biotinylated ligands, to the activated groups (*21*, *23*). Surface-conjugated particles were incubated with neutrophils in whole blood, and their uptake was compared to that of unconjugated particles. Neutrophil phagocytosis of PEG particles activated with EDC decreased significantly compared to unconjugated ones for the 2-μm 50 and 15% PEG formulations. As shown in Fig. 5A, the 50% PEG particle type displayed a significant 1.3-fold reduction in uptake when comparing EDC-activated particles

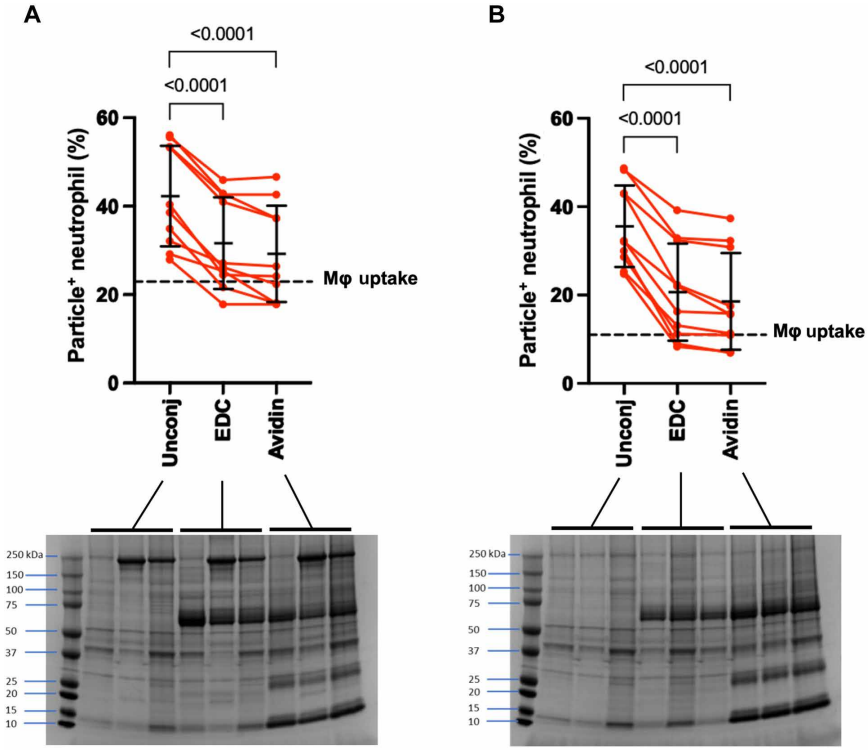

Fig. 5. Uptake of surface-conjugated PEG particles. The 2-μm-sized (**A**) 50% and (**B**) 15% PEG particles either unconjugated (Unconj), activated with EDC, or covalently coated with avidin were incubated with primary human neutrophils in whole blood. The data average is shown as a horizontal check with error bars. The set of three data represent plasma from three distinct donors. For comparison, the dotted line on each graph represents the average uptake of each respective particle type by J774 macrophages at a ratio of 40 particles per cell. The protein coronas of these particles were also visualized using SDS–polyacrylamide gel electrophoresis (PAGE) and stained with Coomassie Blue. There were notable bands for both EDC activation and avidin coating around 60 kDa. Statistics for phagocytosis assays were performed using repeated measures of one-way ANOVA with Dunnett's multiple comparisons test. Error bars represent SD with $n = 10$ independent blood donors.

to an unconjugated control. This decrease in PEG particle uptake with EDC activation was not eliminated with the surface coupling of avidin protein to the activated groups on particles. The avidin-coated 50% PEG particles had a 1.4-fold decrease in particle uptake compared to an unconjugated control. Similarly, when comparing EDC-activated and avidin-coated 15% PEG particles to an unconjugated control, we observed a significant 1.7- and 1.9-fold decrease in neutrophil phagocytosis, respectively (Fig. 5B). The dotted line in Fig. 5 (A and B) corresponds to the average uptake of the corresponding unconjugated PEG particle by J774 macrophages shown previously, demonstrating that this reduction in neutrophil uptake due to surface conjugation is not as pronounced as the reduced uptake observed when macrophages try to engulf elastic particles relative to rigid PS counterpart, even at considerable ratios of PEG particles to macrophages.

On the basis of the data in the prior figures, we determined that apparent differences in uptake after EDC conjugation were likely not linked to differences in particle deformability, given all our PEG formulations having similar levels of uptake by neutrophils (Fig. 1, A and B), as well as we confirmed that neutrophils can phagocytose PEG particles of various zeta potential (Fig. 4). Thus, to account for these differences in particle uptake with EDC conjugation, we next looked at any differences in protein adsorption, which have been strongly correlated with particle recognition and phagocytosis. Using SDS–polyacrylamide gel electrophoresis (PAGE) to analyze the protein corona of the particles, we found distinct bands on both the EDC-activated and avidin-conjugated PEG particles, which were not present on the unconjugated control, specifically around 60 kDa. Given albumin makes up 50 to 60% of plasma proteins and has a molecular weight of 66 kDa, we hypothesize that EDC coupling increases albumin absorption on the surface of the PEG hydrogels (*46*, *47*). We further analyzed the 60-kDa bands using ImageJ to quantify the band intensity (*39*) and found no differences between the band intensity of EDC- and avidin-modified 50 and 15% PEG particles. However, both EDC- and avidin-coated particles had significantly more albumin than the unconjugated PEG hydrogels, which likely explains their lower uptake by human neutrophils (fig. S7).

To determine whether this differential protein adsorption with conjugation is linked to the EDC chemistry, we incubated PEG particles coated with avidin using thiol-ene click chemistry, circumventing the use of EDC. As shown in fig. S8, when EDC was removed from the coupling process, we did not observe differences in neutrophil uptake of avidin-coated particles compared to that of an unconjugated control. These data were further supported by the similarities in protein corona between the two particle types.

In summary, we find that protein absorption to the PEG particle surface depends on the conjugation strategy used to attach biotinylated ligands for vascular targeting. Both approaches have implications for the efficacy of targeting particles to disease areas by either enhancing or preventing phagocytic interactions with neutrophils in blood flow.

In vivo biodistribution and uptake of particles in BALB/c mice

Thus far, all phagocytosis assays have been done in an ex vivo setting. To investigate how these particles might behave in an in vivo setting, we injected 1.75-μm PS and 2-μm 50% PEG microparticles into male BALB/c mice. We measured the biodistribution of particles and the percentage of particles remaining in circulation in blood after the 2-hour assay. Figure 6A shows PS and 50% PEG microparticles localized in different organs in BALB/c mice. The PS

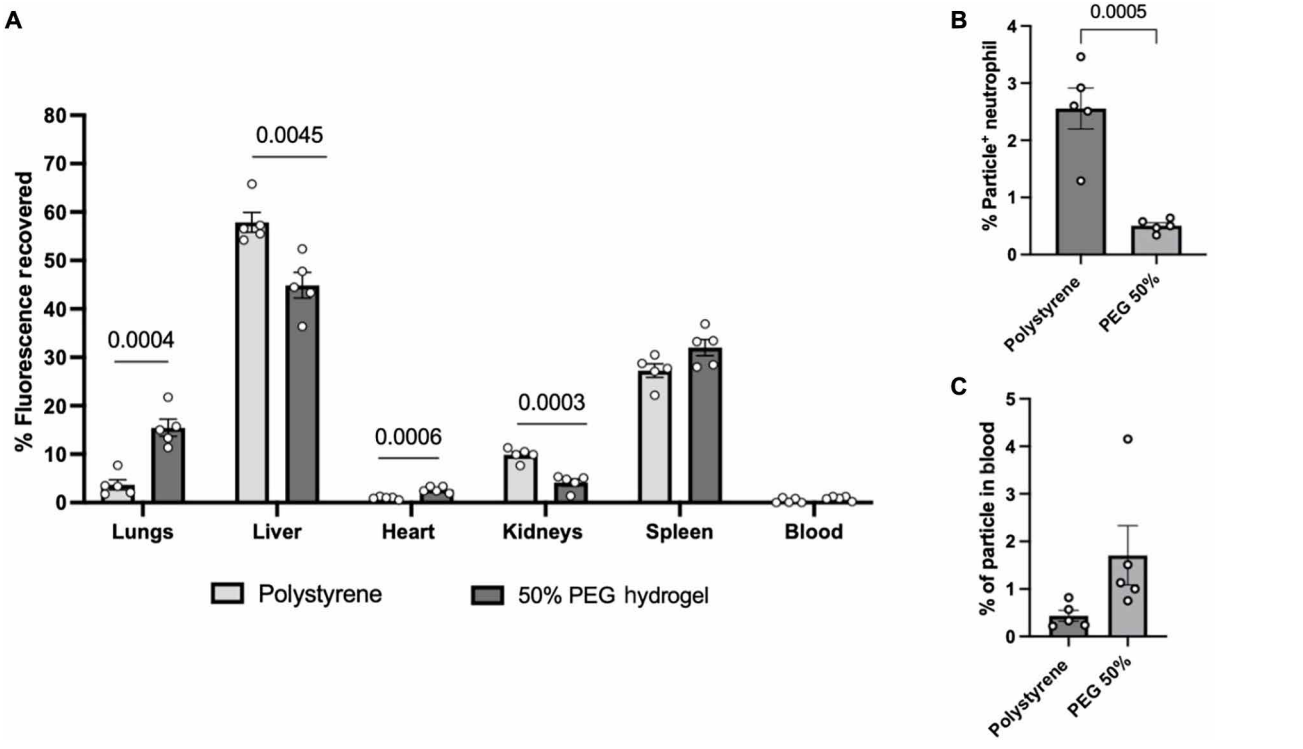

Fig. 6. Biodistribution of PS and 50% PEG particles in BALB/c mice. (**A**) Biodistribution of 1.75-μm PS or 2-μm 50% PEG hydrogels after 2 hours intravenous injection of male BALB/c mice. (**B**) In vivo uptake of PS and PEG particles by mouse neutrophils, quantified as a percentage of particle-positive neutrophils. (**C**) Particles remaining in circulation 2 hours after injection, quantified as a percentage of particles relative to the number of white blood cells. Statistics were performed using Student's *t* test for all plots with $n = 5$ male mice.

particles were primarily found in the liver and spleen, while the PEG particles were localized in the liver, spleen, and, to a lesser extent, the lungs. Notably, there was a significant difference in the localization of particles in the lungs, liver, heart, and kidneys. Similar results were found when we injected PS and PEG particles in female BALB/c (fig. S9). Analysis of the blood was also done after the 2-hour assay. As shown in Fig. 6B, the levels of particle-positive neutrophils overall were very low, ranging between 0.5 and 3.5%. However, there were significant differences between PS and PEG levels of particle-positive neutrophils remaining in the blood, with a fivefold decrease in the PEG particles compared to that in PS.

In addition, we looked at the percentage of particles remaining in circulation after 2 hours. As shown in Fig. 6C, both particle types were effectively removed from the blood by the 2-hour mark, with only 0.5 to 2% of injected particles remaining for both types. Although slightly more PEG particles remained in the blood than the PS, this difference was not significant.

DISCUSSION

The current literature regarding phagocytosis of particles by immune cells has primarily focused on macrophages and monocytes, with few papers exploring the use of neutrophils, likely due to difficulties in obtaining fresh neutrophils combined with a lack of reliable neutrophil-like cell lines for culture. As more studies look at interactions between particles and neutrophils, differences in their phagocytic behavior relative to other immune cells have begun to arise. For example, a study by Kelley *et al.* (*17*) showed that PEGylation of particles can cause enhanced phagocytosis by primary human neutrophils in human blood instead of reducing uptake, as seen with Tohoku Hospital Pediatrics-1 (THP-1) monocytes and bone marrow–derived macrophages from mice. Similarly, a study by Safari *et al.* (*18*) saw notably higher phagocytosis of rod-shaped particles by neutrophils than spheres compared to rat alveolar macrophages and primary human monocytes. These studies emphasize the critical need for the characterization of neutrophil interactions with particle carriers, which have, to date, been understudied. Thus, we sought to determine whether cell-particle interactions between neutrophils and particles of different elasticities would depart from accepted trends in the literature regarding phagocytosis by macrophages and monocytes.

On the basis of the vast amount of literature on interactions between immune cells and particles of varying moduli, we expected to see a reduction in uptake as we moved from a rigid PS control to softer PEG-derived particles. Instead, neutrophils were as likely or more likely to phagocytose PEG- and HA-based particles compared to the non-deformable PS. Our data suggests that modulus may not be as effective of a parameter to leverage when designing carriers to avoid particle clearance from the bloodstream in humans, where neutrophils are likely the first phagocytes encountered by intravenously delivered particles. We hypothesize that these differences in uptake between neutrophils and other phagocytes may arise from the deformation of the PEG particles as they undergo membrane wrapping by neutrophils, resulting in an enhanced phagocytosis effect due to an apparent elongated particle shape as the particle is engulfed (*37*). Given the relevance of nanoparticles compared to microparticles in current vascular delivery technologies, our results indicate that deformable nanoparticles might experience a similar loss of efficacy as rigid nanoparticles, given their similar propensity for neutrophil clearance. We also note that micron-sized particles have been demonstrated to have a greater propensity for margination and subsequent vascular adhesion to the endothelium (*21*, *23*). However, the higher risk of occlusive events likely renders them unusable in the clinic. Considering these findings, deformable micron-sized particles may overcome these challenges due to the particles' deformability (*1*, *23*). However, micro-sized hydrogels might experience a similar phagocytic clearance fate as nano-sized carriers and rigid particles.

Similarly, we see a reduction in deformable particle uptake by J774 macrophages because of their reported inability to effectively phagocytose rod-like particles, which has been linked to a higher energy barrier of membrane wrapping (*48*, *49*). Our study demonstrates that J774 macrophages exhibited significantly higher uptake of rigid particles compared to both PEG and HA hydrogels. We observed that a greater percentage of macrophages internalized HA hydrogels than PEG particles, despite both having similar Young's moduli, suggesting that particle chemistry, alongside elasticity, may play a role in the phagocytic activity of macrophages. In contrast, neutrophils showed comparable uptake levels for both HA and PEG particles, indicating that they can effectively engulf particles regardless of elasticity or chemical composition. This difference underlines potentially distinct mechanisms of particle uptake between macrophages and neutrophils.

We did not observe significant deformation of the PEG particles when engulfed by both neutrophils in our optical tweezer assay, although prior studies successfully imaged particle deformation with macrophages phagocytosing notably stiffer particles that used here, between two and three orders of magnitude higher (*36*). Our inability to visualize any changes in particle shape during the engulfment process with our optical tweezer system may be due to the use of micron-sized particles because of instrument limitations, as opposed to nano-sized particles with prior studies. It is also possible that the lack of shape change with neutrophil phagocytosis may be linked to differences in forces exerted by macrophages and neutrophils. Considering that the PEG particle detached from the macrophage after the tweezer assay was complete, the lack of phagocytosis may also be linked to their inability to adhere to the particle and energetic barriers to the membrane wrapping of a deformable particle. One modification that may be used in future imaging studies is use of flipper dyes incorporated into the particle matrix, which would allow for more sensitive measurements of particle deformation than visual shape changes. Furthermore, the ability to image nanoparticles during phagocytosis would help to elucidate the mechanism by which we see this enhanced phagocytosis of deformable particles, as well as further characterization of the biomechanics of neutrophil phagocytosis.

Past literature has reported that mouse peritoneal macrophages effectively took up both negatively and positively charged cellulose-derived particles. In contrast, a neutrally charged particle exhibited a sharp reduction in uptake (*38*). Many studies have accordingly leveraged this phenomenon to modulate zeta potential, notably with zwitterionic coatings, to reduce or eliminate the protein corona and thereby avoid immune cell recognition (*5*, *6*, *50*). Given the implications of zeta potential on plasma protein adsorption and observed behavior with macrophages, we predicted a similar reduction in uptake at a neutral charge with neutrophils in whole blood. However, the unexpectedly equal uptake of 2-μm 50% PEG particles observed across all charges suggests that competing forces may affect neutrophil uptake. While a neutral charge typically lowers phagocytosis,

our findings indicate that a deformable particle is also more likely to be taken up by neutrophils, which may explain the lack of reduced uptake. Similar results obtained when using isolated neutrophils in serum-free medium support our hypothesis that these observations are linked to deformability as opposed to any differences in protein corona.

Because VTCs typically are functionalized with targeting ligands for adhesion to cellular markers and co-localized with circulating neutrophils in blood flow, we also investigated the effects of surface modification on neutrophil phagocytosis. Previous studies have indicated that surface functionalization enhances phagocytosis. Yet, the decrease in neutrophil uptake suggests that these modifications to the particle surface may help evade immune cell clearance when delivered intravenously if following EDC coupling (*51*, *52*). After running SDS-PAGE, we saw a distinct band at the 60-kDa mark for the EDC-conjugated particles that were not present on unconjugated particles. Given the molecular weight, this protein is likely albumin, a highly prevalent plasma protein. Albumin, a dysopsonin, has been shown to protect particles from immune cell recognition and clearance and may cause the reduced phagocytosis observed in neutrophils (*53*–*56*). Overall, we find that there may still be concerns with enhanced phagocytosis of deformable particles by neutrophils despite the modest reduction in uptake upon EDC-based surface conjugation, given that this albumin-driven reduction did not achieve the more marked decrease in uptake of deformable particles seen in macrophages.

Because all the trends in phagocytosis with deformable particles, thus far, have been in ex vivo human neutrophils, the in vivo data in Fig. 6 complement these data. The differences in organ localization seen in the BALB/c mouse biodistribution data can largely be attributed to differences in particle rigidity, as softer particles will be less likely to be filtered out by these RES organs (kidney, liver, and spleen) (*9*, *57*). Notably, a massive fraction (>98%) of both PS and PEG particles injected particles were effectively cleared from circulation, highlighting effective particle phagocytosis by neutrophils regardless of deformability. Given the more prominent presence of neutrophils in systemic circulation, we expect that this observation will be exaggerated in humans. The data regarding the percentage of particle-positive neutrophils remaining in the blood may suggest higher PS uptake and appear to contradict our earlier data, indicating increased uptake of PEG particles in an ex vivo setting. However, this difference may be more due to the diversion patterns of particle-positive cells from circulation to the RES organs than the uptake differences (*58*).

One limitation of this work is that assays with human blood were conducted under static conditions. Although microfluidic assays can be used to study particle uptake under flow conditions, they may not fully represent the in vivo setting, especially for particles injected intravenously into flowing blood. A recent study explored the effect of flow conditions during the phagocytic uptake of PS particles by primary human neutrophils, showing that human neutrophils can more efficiently uptake particles in moderate flow conditions than in static environments (*59*). However, incubating particles with cells or whole blood before flowing the mixture into a fluidic channel may not capture the unique cellular distribution and cell-particle interactions in blood flow, which are likely to affect particle uptake under flow conditions. The slight differences in particle phagocytosis and in vivo circulation time between PEG and PS may be influenced by differences in collision between softer particles and circulating neutrophils. Particle margination is influenced by elastic collisions with red blood cells, which push them toward the endothelial wall (*60*). The softer PEG particles likely participate in more inelastic collisions, reducing their propensity to localize to the cell-free layer, where these circulating neutrophils are typically present. Thus, an important future work would be to develop realistic in vitro blood flow assays that can visualize the phagocytic ability of neutrophils for deformable particles underflow.

Our work seeks to advance our understanding of interactions between particle drug carriers and neutrophils, which historically have not been as well characterized as macrophages and monocytes, especially in vascular drug delivery. Our results here suggest that the reported benefits of deformable particles, including longer circulation times and more effective avoidance of clearance by tissue-resident macrophages and monocytes, may not hold with respect to neutrophils. We find that a deformable particle instead exhibits an enhanced or similar phagocytic effect as rigid particles, which might undermine efforts to improve vascular-targeted drug delivery. Work in this space will need to explore further the potential interplay between deformability and other design parameters, such as density and shape. Our results here also highlight the possible shortcomings of mouse models and cell lines, which may be less physiologically relevant with respect to neutrophils and vascular drug delivery, along with a need for further characterization of neutrophils and their interactions with particle drug carriers.

MATERIALS AND METHODS

Experimental design

Our experiments were designed to investigate the effect of particle elasticity on the association of hydrogel particles with different types of phagocytes. PEG and HA particles of varying elastic moduli were fabricated by adjusting the polymer concentration, and their association with neutrophils and macrophages was quantified. Particles were modified with surface conjugation or altered zeta potential to assess interplay between these parameters and particle deformability. All the human donors for the experiments were healthy. The animal blood was collected from healthy mice. In vivo experiments were performed on healthy mice. All the experiments were replicated at least three times.

Study approvals

We obtained written informed consent from all human blood donors before blood draws according to a protocol (no. HUM00013973) approved by the University of Michigan Internal Review Board. Both male and female donors, aged 18 to 49, were included. All participants were monetarily compensated for their blood donation.

All animal studies followed the National Institute of Health's *Guide for the Care and Use of Laboratory Animals* and protocol (no. PRO00010572) approved by the University of Michigan Institutional Animal Care and Use Committee. BALB/c mice were obtained from the Jackson Laboratory. All mice were housed under specific pathogen–free conditions and maintained at the University of Michigan in compliance with the University Committee on Use and Care of Animal regulations.

Particle fabrication

PEG particles were fabricated as previously described (*23*). We first mixed PEG diacrylate (PEGDA), CEA, lithium phenyl (2,4,6-trimethylbenzoyl) phosphinate (LAP), acryloxyethyl thiocarbamoyl

rhodamine B, and methanol to form a precursor solution, with PEGDA in quantities to create 50, 40, 20, and 15 wt % solutions. The precursor solution was then added to an oil phase of silicone oil in 1-to-10 volumetric ratios, briefly sonicated to form a water-in-oil emulsion, and placed under an ultraviolet (UV) lamp to allow particles to cross-link. Particles were washed in hexanes and ethanol and filtered using 2-μm filters. To alter the zeta potential of the PEG particles, an equivalent mass of AEM was added instead of the CEA. Neutrally charged 15% PEG particles were fabricated using an equivalent mass of a 50:50 mixture of CEA and AEM and a 35:65 (CEA:AEM) mixture for neutrally charged 50% PEG particles. Successful AEM incorporation into the particle backbone was demonstrated using a fluorescamine assay.

HA-based hydrogels were fabricated similarly to PEG hydrogels. First, a HAMA precursor solution comprising 2% rhodamine, 5% LAP, 10% CEA, and varying wt % of HA (5, 8, and 10% w/v) in deionized (DI) water was made. The HA precursor solution was then added to silicone oil, sonicated to form a water-in-oil emulsion, and placed under a UV lamp for particles to cross-link. Particles were washed in hexanes and ethanol and filtered using 2-μm filters.

Particles used here were analyzed using scanning electron microscopy to visualize their morphology and size. At least 50 particles were measured using ImageJ to determine their diameter. Results are shown as the average particle diameter ± SD. Likewise, we used a Zetasizer to measure the particles' zeta potential.

Cell culture

J774 macrophages were purchased from the American Type Culture Collection (ATCC) and cultured according to a protocol by ATCC. The cell vial was first thawed and resuspended in 10 ml of Dulbecco's modified Eagle's medium (DMEM) supplemented with 10% fetal bovine serum (FBS) and then centrifuged at 250*g* for 5 min. After removing the supernatant, the cells were resuspended in 10 ml of fresh DMEM, transferred to a T75 flask, and incubated at 37°C and 5% CO_2. Medium was replaced every 2 days, and cells were subcultured every 5 days by removing spent medium from the flask via aspiration and adding 10 ml of fresh medium. Next, cells were detached from the flask using a cell scraper, and the cell suspension was transferred to new T75 flasks at a 1:3 dilution of cells to fresh medium. For particle uptake studies, cells were first detached from T75 flasks and counted using a hemacytometer. Cells were then centrifuged at 250*g* and reconstituted with fresh medium to a concentration of 10^6 cells/ml for future use.

Neutrophil isolation

Fresh human blood (20 ml) was first drawn from a healthy human donor, layered onto a Lymphoprep density gradient in a 1:1 volume ratio, and centrifuged at 400*g* for 20 min. The plasma layer was collected for future use, and the supernatant (buffy coat and gradient layer) was discarded. 20% dextran with 0.15 M NaCl was added to the RBC and neutrophil layer at a 1:2 volume ratio and mixed by gently rotating the tube. Phosphate-buffered saline $(PBS)^{-/-}$ was added up to 25 ml of total volume, the tube was gently rotated, and the RBCs were allowed to settle for 30 min. The supernatant (neutrophils and residual RBCs) was collected, and $PBS^{-/-}$ was added up to 50 ml and centrifuged at 500*g* for 5 min. The supernatant was then aspirated, and, to lyse the remaining RBCs, 20 ml of 0.2% NaCl solution was first added and mixed by inverting. After 45 s, 30 ml of 1.8% NaCl solution was added to the tube and centrifuged at 500*g* for 5 min. Cells were washed once with $PBS^{-/-}$, counted, and resuspended in plasma or RPMI medium for future assays. As shown in fig. S10, the purity of the isolated neutrophil sample was confirmed using flow cytometry and determined by $CD45^+CD66b^+$ cells.

Particle uptake studies

Ex vivo human blood uptake assays

Fresh blood was drawn from a healthy human donor, and 100 μl of whole blood each was placed into fluorescence-activated cell sorting (FACS) tubes for particle uptake assays. Particles were added to each tube for a final concentration of 10^7 particles/ml of whole blood for 2-μm particles or 10^8 particles/ml for 500-nm particles. Samples were incubated at 37°C and 5% CO_2 for 2 hours. Afterward, on ice, neutrophils were stained with allophycocyanin (APC)–CD45 and APC-Cy7-CD11b for 30 min before cell fixing with Fix-Lyse buffer to remove red blood cells. Samples were subjected to centrifugal washes before analysis using flow cytometry. Immune cells comprised events positive for CD45 and CD11b, and neutrophils were identified using CD45 (BioLegend, no. 368512) and $CD11b^+$ (BioLegend, no. 301342) gates and forward and side scatter panels. Particle-positive cells were ones positive for fluorescein isothiocyanate (FITC)–labeled PS particles and rhodamine-labeled PEG- and HA-based hydrogels. For isolated neutrophils, 2×10^5 cells in 100 μl of either RPMI medium were placed in FACS tubes per sample, and 10^6 particles were placed in each sample for a cell:particle ratio of 1:5. The uptake study was then run as with whole blood samples. At least 5000 events were recorded for each assay to ensure a sufficient population for uptake analysis.

J774 macrophage uptake assays

Cells were first detached from T75 flasks via scraping, followed by counting cells using a hemacytometer to determine cell concentration. Cells were centrifuged at 250*g* and resuspended at 10^6 cells/ml of DMEM medium with 10% FBS. Next, 10^5 cells per sample were placed in the wells of a 96-well plate and incubated at 37°C and 5% CO_2 to allow the cells to adhere to the plate. Afterward, 4×10^6 particles were added per sample for 2-μm PEG- and HA- hydrogels and 5×10^7 particles for 500-nm PEG hydrogels. Cells were incubated with particles for 2 hours to allow for phagocytosis. Macrophages were detached by gently pipetting the medium up and down, followed by cell fixation with 2% paraformaldehyde. Samples were analyzed with flow cytometry, and results were represented as a percentage of particle-positive cells from the whole population. At least 5000 events were recorded for each assay to ensure a sufficient population for uptake analysis.

Ex vivo mouse blood uptake

Mouse blood from BALB/c mice (male, 3 to 4 weeks) was obtained via cardiac puncture. Heparinized mouse blood (100 μl) was incubated with particles at 10^7 particles/ml of blood for 2 hours for phagocytosis. Samples were analyzed using flow cytometry to determine particle-positive mouse neutrophils via the following antibodies: FITC CD11b (BioLegend, no. 101206), BV605-Ly6G (BioLegend, no. 127639), and BV421-Ly6C (BioLegend, no. 128032). At least 5000 events were recorded for each assay to ensure a sufficient population for uptake analysis.

Single-cell-particle optical tweezer imaging

First, poly-L-lysine (1 mg/ml) was adsorbed to cover glass-bottom cell culture dishes (Bioptechs) for 5 min before rinsing with DI H_2O. Cells (1 ml; either primary human neutrophils or J774 macrophages) were added (diluted in plasma to ~ 1.6×10^6 cells/ml) and

allowed 15 min to adhere. Particles (100 μl) were added to the dish, and the dish was mounted on a temperature-controlled stage (Bioptechs) to maintain the sample at 37°C throughout the experiment.

Particles were manipulated using a bespoke optical tweezer system. Briefly, a 1064-nm laser (IPG Photonics) was expanded to slightly overfill the back aperture of an objective (Nikon MRD01602, 60×, 1.45 numerical aperture) and then focused to a diffraction-limited spot at the image plane. Particles were optically trapped and brought into contact with a cell. Images of the cells were acquired with bright-field images at ~1 Hz, and the cell was then observed over 5 min to assess particle engulfment.

Bulk hydrogel rheometry

Briefly, a hydrogel polymer precursor solution was made, as described previously. The polymer solution was placed between two hydrophobic coverslips, spaced 1.25 mm apart for PEG hydrogels and 1 mm apart for HA hydrogels, to form disk-shaped bulk samples. Next, the solution was cross-linked using a UV lamp and allowed to swell for 30 min. Round samples (8-mm diameter) were then cut out of the hydrogel sample and stored in PBS overnight for rheometry analysis.

To determine Young's modulus of our hydrogel materials, we placed our disk samples on the heated stage of an ARG2 rheometer for PEG hydrogels and a DHR3 rheometer for HA hydrogels and held at 37°C and used an 8-mm plate geometry for rheometry. The normal force during each measurement was kept at 0.5 N, and a time sweep was performed using a 1% strain and an angular frequency of 1 rad/s. These assays yielded a storage modulus, which was then converted to Young's modulus by assuming a Poisson's ratio of 0.5 for elastic materials.

Confocal microscopy

Neutrophils were first isolated and incubated with either 2-μm PS, 50% PEG, or 15% PEG particles at a cell/particle ratio of 1:5 for 2 hours. After incubation, cells were fixed with 2% paraformaldehyde (PFA) for 1 hour and washed three times. Before imaging, the neutrophil cell membrane was stained with wheat germ agglutinin (Alexa Fluor 633) and plated on a poly-L-lysine–coated 96-well plate. Particles were then imaged using a confocal microscope to assess particle internalization.

Particle biodistribution in BALB/c mice

For in vivo experiments, DyLight 680 maleimide dye was conjugated to 2-μm 50% PEG particles instead of rhodamine dye. For PS, we used 1.75-μm PS with a near-IR dye from PolySciences. Male and Female BALB/c mice (the Jackson Laboratory, 3 to 4 weeks) were anesthetized using isoflurane, and 50 μl of 4×10^9 particles were injected via retro-orbital injection. Two hours after injection, mice were euthanized, and blood was collected via cardiac puncture. Organs, including the lungs, liver, kidneys, spleen, and heart, were harvested and stored in PBS on ice until scanned. Mouse blood was stained with CD11b, Ly6G, and Ly6C, and the percentage of particle-positive mouse neutrophils and particles remaining in blood was quantified using flow cytometry.

Whole-organ scans were performed on an Odyssey CLx Infrared Imaging System using the 700-nm channel. Total fluorescence revered from each organ was determined by drawing a region of interest using Image Studio Software from LI-COR. Untreated samples were used to determine the background fluorescence for each organ, which was subtracted from the fluorescence obtained for each organ region of interest.

Statistical analysis

Statistical analysis of the data was performed using GraphPad Prism. Each data point was replicated in at least triplicate. Data were analyzed using either an unpaired Student's *t* test or one-way analysis of variance (ANOVA) with Tukey's multiple comparisons tests, or Dunnett's multiple comparisons test, depending on the dataset. All error bars represent the SEM.

Supplementary Materials

The PDF file includes:

Figs. S1 to S10
Tables S1 and S2
Legends for movies S1 and S2

Other Supplementary Material for this manuscript includes the following:

Movies S1 and S2

REFERENCES AND NOTES

1. M. B. Fish, A. L. Banka, M. Braunreuther, C. A. Fromen, W. J. Kelley, J. Lee, R. Adili, M. Holinstat, O. Eniola-Adefeso, Deformable microparticles for shuttling nanoparticles to the vascular wall. *Sci. Adv.* **7**, eabe0143 (2021).
2. J. Key, A. L. Palange, F. Gentile, S. Aryal, C. Stigliano, D. Di Mascolo, E. De Rosa, M. Cho, Y. Lee, J. Singh, P. Decuzzi, Soft discoidal polymeric nanoconstructs resist macrophage uptake and enhance vascular targeting in tumors. *ACS Nano* **9**, 11628–11641 (2015).
3. T. J. Merkel, S. W. Jones, K. P. Herlihy, F. R. Kersey, A. R. Shields, M. Napier, J. C. Luft, H. Wu, W. C. Zamboni, A. Z. Wang, J. E. Bear, J. M. DeSimone, Using mechanobiological mimicry of red blood cells to extend circulation times of hydrogel microparticles. *PNAS* **108**, 586–591 (2011).
4. T. J. Merkel, K. Chen, S. W. Jones, A. A. Pandya, S. Tian, M. E. Napier, W. E. Zamboni, J. M. DeSimone, The effect of particle size on the biodistribution of low-modulus hydrogel PRINT particles. *J. Control. Release* **162**, 37–44 (2012).
5. L. Zhang, Z. Cao, Y. Li, J.-R. Ella-Menye, T. Bai, S. Jiang, Softer zwitterionic nanogels for longer circulation and lower splenic accumulation. *ACS Nano* **6**, 6681–6686 (2012).
6. K. Pombo García, K. Zarschler, L. Barbaro, J. A. Barreto, W. O'Malley, L. Spiccia, H. Stephan, B. Graham, Zwitterionic-coated "stealth" nanoparticles for biomedical applications: Recent advances in countering biomolecular corona formation and uptake by the mononuclear phagocyte system. *Small* **10**, 2516–2529 (2014).
7. C.-M. J. Hu, L. Zhang, S. Aryal, C. Cheung, R. H. Fang, L. Zhang, Erythrocyte membrane-camouflaged polymeric nanoparticles as a biomimetic delivery platform. *Proc. Natl. Acad. Sci. U.S.A.* **108**, 10980–10985 (2011).
8. R. H. Fang, A. V. Kroll, W. Gao, L. Zhang, Cell membrane coating nanotechnology. *Adv. Mater.* **30**, e1706759 (2018).
9. A. C. Anselmo, M. Zhang, S. Kumar, D. R. Vogus, S. Menegatti, M. E. Helgeson, S. Mitragotri, Elasticity of nanoparticles influences their blood circulation, phagocytosis, endocytosis, and targeting. *ACS Nano* **9**, 3169–3177 (2015).
10. M. Yildirim, A.-V. Weiss, M. Schneider, The effect of elasticity of gelatin nanoparticles on the interaction with macrophages. *Pharmaceutics* **15**, 199 (2023).
11. A. C. Anselmo, S. Mitragotri, Impact of particle elasticity on particle-based drug delivery systems. *Adv. Drug Deliv. Rev.* **108**, 51–67 (2017).
12. K. A. Beningo, Y.-L. Wang, Fc-receptor-mediated phagocytosis is regulated by mechanical properties of the target. *J. Cell Sci.* **115**, 849–856 (2002).
13. M. Li, X. Jin, T. Liu, F. Fan, F. Gao, S. Chai, L. Yang, Nanoparticle elasticity affects systemic circulation lifetime by modulating adsorption of apolipoprotein A-I in corona formation. *Nat. Commun.* **13**, 4137 (2022).
14. J. Tao, W. Shi, K. Chen, W. Lu, A. J. Elbourne, L. Bao, L. Weng, X. Zheng, X. Su, Z. Teng, L. Wang, Elasticity of mesoporous nanocapsules regulates cellular uptake, blood circulation, and intratumoral distribution. *Biomater. Sci.* **11**, 822–827 (2023).
15. M. Müllner, S. J. Dodds, T.-H. Nguyen, D. Senyschyn, C. J. H. Porter, B. J. Boyd, F. Caruso, Size and rigidity of cylindrical polymer brushes dictate long circulating properties in vivo. *ACS Nano* **9**, 1294–1304 (2015).
16. C.-H. Wu, T.-D. Wang, C.-H. Hsieh, S.-H. Huang, J.-W. Lin, S.-C. Hsu, H.-T. Wu, Y.-M. Wu, T.-M. Liu, Imaging cytometry of human leukocytes with third harmonic generation microscopy. *Sci. Rep.* **6**, 37210 (2016).

17. W. J. Kelley, C. A. Fromen, G. Lopez-Cazares, O. Eniola-Adefeso, PEGylation of model drug carriers enhances phagocytosis by primary human neutrophils. *Acta Biomater.* **79**, 283–293 (2018).
18. H. Safari, W. J. Kelley, E. Saito, N. Kaczorowski, L. Carethers, L. D. Shea, O. Eniola-Adefeso, Neutrophils preferentially phagocytose elongated particles—An opportunity for selective targeting in acute inflammatory diseases. *Sci. Adv.* **6**, eaba1474 (2020).
19. K. Namdee, M. Carrasco-Teja, M. B. Fish, P. Charoenphol, O. Eniola-Adefeso, Effect of Variation in hemorheology between human and animal blood on the binding efficacy of vascular-targeted carriers. *Sci. Rep.* **5**, 11631 (2015).
20. P. Charoenphol, S. Mocherla, D. Bouis, K. Namdee, D. J. Pinsky, O. Eniola-Adefeso, Targeting therapeutics to the vascular wall in atherosclerosis–carrier size matters. *Atherosclerosis* **217**, 364–370 (2011).
21. P. Charoenphol, R. B. Huang, O. Eniola-Adefeso, Potential role of size and hemodynamics in the efficacy of vascular-targeted spherical drug carriers. *Biomaterials* **31**, 1392–1402 (2010).
22. T.-R. Lee, M. Choi, A. M. Kopacz, S.-H. Yun, W. K. Liu, P. Decuzzi, On the near-wall accumulation of injectable particles in the microcirculation: Smaller is not better. *Sci. Rep.* **3**, 2079 (2013).
23. M. B. Fish, C. A. Fromen, G. Lopez-Cazares, A. W. Golinski, T. F. Scott, R. Adili, M. Holinstat, O. Eniola-Adefeso, Exploring deformable particles in vascular-targeted drug delivery: Softer is only sometimes better. *Biomaterials* **124**, 169–179 (2017).
24. D. Guo, J. Li, G. Xie, Y. Wang, J. Luo, Elastic properties of polystyrene nanospheres evaluated with atomic force microscopy: Size effect and error analysis. *Langmuir* **30**, 7206–7212 (2014).
25. X. Yi, X. Shi, H. Gao, Cellular uptake of elastic nanoparticles. *Phys. Rev. Lett.* **107**, 098101 (2011).
26. J. F. Alexander, V. Kozlovskaya, J. Chen, T. Kuncewicz, E. Kharlampieva, B. Godin, Cubical shape enhances the interaction of layer-by-layer Polymeric particles with breast cancer cells. *Adv. Healthc. Mater.* **4**, 2657–2666 (2015).
27. T. J. Beldman, M. L. Senders, A. Alaarg, C. Pérez-Medina, J. Tang, Y. Zhao, F. Fay, J. Deichmöller, B. Born, E. Desclos, N. N. van der Wel, R. A. Hoebe, F. Kohen, E. Kartvelishvily, M. Neeman, T. Reiner, C. Calcagno, Z. A. Fayad, M. P. J. de Winther, E. Lutgens, W. J. M. Mulder, E. Kluza, Hyaluronan nanoparticles selectively target plaque-associated macrophages and improve plaque stability in atherosclerosis. *ACS Nano* **11**, 5785–5799 (2017).
28. L. Messager, N. Portecop, E. Hachet, V. Lapeyre, I. Pignot-Paintrand, B. Catargi, R. Auzély-Velty, V. Ravaine, Photochemical crosslinking of hyaluronic acid confined in nanoemulsions: Towards nanogels with a controlled structure. *J. Mater. Chem. B* **1**, 3369–3379 (2013).
29. D. Nikjoo, I. van der Zwaan, M. Brülls, U. Tehler, G. Frenning, Hyaluronic acid hydrogels for controlled pulmonary drug delivery—A particle engineering approach. *Pharmaceutics* **13**, 1878 (2021).
30. S. K. Seidlits, Z. Z. Khaing, R. R. Petersen, J. D. Nickels, J. E. Vanscoy, J. B. Shear, C. E. Schmidt, The effects of hyaluronic acid hydrogels with tunable mechanical properties on neural progenitor cell differentiation. *Biomaterials* **31**, 3930–3940 (2010).
31. B. S. Spearman, N. K. Agrawal, A. Rubiano, C. S. Simmons, S. Mobini, C. E. Schmidt, Tunable methacrylated hyaluronic acid-based hydrogels as scaffolds for soft tissue engineering applications. *J. Biomed. Mater. Res. A* **108**, 279–291 (2020).
32. S. Garantziotis, R. C. Savani, Hyaluronan biology: A complex balancing act of structure, function, location and context. *Matrix Biol.* **78–79**, 1–10 (2019).
33. K. S. Anseth, C. N. Bowman, L. Brannon-Peppas, Mechanical properties of hydrogels and their experimental determination. *Biomaterials* **17**, 1647–1657 (1996).
34. D. M. Richards, R. G. Endres, The mechanism of phagocytosis: Two stages of engulfment. *Biophys. J.* **107**, 1542–1553 (2014).
35. M. Herant, V. Heinrich, M. Dembo, Mechanics of neutrophil phagocytosis: Experiments and quantitative models. *J. Cell Sci.* **119**, 1903–1913 (2006).
36. Y. Hui, X. Yi, D. Wibowo, G. Yang, A. P. J. Middelberg, H. Gao, C.-X. Zhao, Nanoparticle elasticity regulates phagocytosis and cancer cell uptake. *Sci. Adv.* **6**, eaaz4316 (2020).
37. J. Sun, L. Zhang, J. Wang, Q. Feng, D. Liu, Q. Yin, D. Xu, Y. Wei, B. Ding, X. Shi, X. Jiang, Tunable rigidity of (polymeric core)–(lipid shell) nanoparticles for regulated cellular uptake. *Adv. Mater.* **27**, 1402–1407 (2015).
38. Y. Tabata, Y. Ikada, Effect of the size and surface charge of polymer microspheres on their phagocytosis by macrophage. *Biomaterials* **9**, 356–362 (1988).
39. G. Lopez-Cazares, O. Eniola-Adefeso, Dual coating of chitosan and albumin negates the protein corona-induced reduced vascular adhesion of targeted PLGA microparticles in human blood. *Pharmaceutics* **14**, 1018 (2022).
40. M. Cui, R. Liu, Z. Deng, G. Ge, Y. Liu, L. Xie, Quantitative study of protein coronas on gold nanoparticles with different surface modifications. *Nano Res.* **7**, 345–352 (2014).
41. S. Honary, F. Zahir, Effect of zeta potential on the properties of nano-drug delivery systems - A review (part 1). *Trop. J. Pharm. Res.* **12**, 255–264 (2013).
42. M. Lundqvist, J. Stigler, G. Elia, I. Lynch, T. Cedervall, K. A. Dawson, Nanoparticle size and surface properties determine the protein corona with possible implications for biological impacts. *Proc. Natl. Acad. Sci. U.S.A.* **105**, 14265–14270 (2008).
43. T. R. Kozel, T. G. McGaw, Opsonization of Cryptococcus neoformans by human immunoglobulin G: Role of immunoglobulin G in phagocytosis by macrophages. *Infect. Immun.* **25**, 255–261 (1979).
44. E. Papini, R. Tavano, F. Mancin, Opsonins and dysopsonins of nanoparticles: Facts, concepts, and methodological guidelines. *Front. Immunol.* **11**, 10.3389/fimmu.2020.567365 (2020).
45. E. R. Brannon, M. V. Guevara, N. J. Pacifici, J. K. Lee, J. S. Lewis, O. Eniola-Adefeso, Polymeric particle-based therapies for acute inflammatory diseases. *Nat. Rev. Mater.* **7**, 796–813 (2022).
46. H. Tao, R. Wang, W. Sheng, Y. Zhen, The development of human serum albumin-based drugs and relevant fusion proteins for cancer therapy. *Int. J. Biol. Macromol.* **187**, 24–34 (2021).
47. J. Mathew, P. Sankar, M. Varacallo, *Physiology, Blood Plasma* (StatPearls Publishing, 2024).
48. J. A. Champion, S. Mitragotri, Role of target geometry in phagocytosis. *Proc. Natl. Acad. Sci. U.S.A.* **103**, 4930–4934 (2006).
49. A. Garapaty, J. A. Champion, Tunable particles alter macrophage uptake based on combinatorial effects of physical properties. *Bioeng. Transl. Med.* **2**, 92–101 (2017).
50. R. R. Arvizo, O. R. Miranda, D. F. Moyano, C. A. Walden, K. Giri, R. Bhattacharya, J. D. Robertson, V. M. Rotello, J. M. Reid, P. Mukherjee, Modulating pharmacokinetics, tumor uptake and biodistribution by engineered nanoparticles. *PLOS ONE* **6**, e24374 (2011).
51. H. Zhong, H. Lin, Q. Pang, J. Zhuang, X. Liu, X. Li, J. Liu, J. Tang, Macrophage ICAM-1 functions as a regulator of phagocytosis in LPS induced endotoxemia. *Inflamm. Res.* **70**, 193–203 (2021).
52. A. Magenau, C. Benzing, N. Proschogo, A. S. Don, L. Hejazi, D. Karunakaran, W. Jessup, K. Gaus, Phagocytosis of IgG-coated polystyrene beads by macrophages induces and requires high membrane order. *Traffic* **12**, 1730–1743 (2011).
53. H. Beukers, F. A. Deierkauf, C. P. Blom, M. Deierkauf, J. C. Riemersma, Effects of albumin on the phagocytosis of polysterene spherules by rabbit polymorphonuclear leucocytes. *J. Cell. Physiol.* **97**, 29–36 (1978).
54. K. Furumoto, J.-I. Yokoe, K. Ogawara, S. Amano, M. Takaguchi, K. Higaki, T. Kai, T. Kimura, Effect of coupling of albumin onto surface of PEG liposome on its in vivo disposition. *Int. J. Pharm.* **329**, 110–116 (2007).
55. Q. Peng, S. Zhang, Q. Yang, T. Zhang, X.-Q. Wei, L. Jiang, C.-L. Zhang, Q.-M. Chen, Z.-R. Zhang, Y.-F. Lin, Preformed albumin corona, a protective coating for nanoparticles based drug delivery system. *Biomaterials* **34**, 8521–8530 (2013).
56. D. J. Sobczynski, O. Eniola-Adefeso, IgA and IgM protein primarily drive plasma corona-induced adhesion reduction of PLGA nanoparticles in human blood flow. *Bioeng. Transl. Med.* **2**, 180–190 (2017).
57. J. M. Caster, S. K. Yu, A. N. Patel, N. J. Newman, Z. J. Lee, S. B. Warner, K. T. Wagner, K. C. Roche, X. Tian, Y. Min, A. Z. Wang, Effect of particle size on the biodistribution, toxicity, and efficacy of drug-loaded polymeric nanoparticles in chemoradiotherapy. *Nanomedicine* **13**, 1673–1683 (2017).
58. C. A. Fromen, W. J. Kelley, M. B. Fish, R. Adili, J. Noble, M. J. Hoenerhoff, M. Holinstat, O. Eniola-Adefeso, Neutrophil–particle interactions in blood circulation drive particle clearance and alter neutrophil responses in acute inflammation. *ACS Nano* **11**, 10797–10807 (2017).
59. M. Srinivas, P. Sharma, S. Jhunjhunwala, Phagocytic uptake of polymeric particles by immune cells under flow conditions. *Mol. Pharm.* **18**, 4501–4510 (2021).
60. P. Charoenphol, P. J. Onyskiw, M. Carrasco-Teja, O. Eniola-Adefeso, Particle-cell dynamics in human blood flow: Implications for vascular-targeted drug delivery. *J. Biomech.* **45**, 2822–2828 (2012).

Acknowledgments

Funding: We thank NSF MRI-ID grant DBI-0959823 for seeding the SMART Center. This work was funded, in part, by the National Science Foundation Graduate Research Fellowship to J.K.L. and M.V.G., a National Institute of Health grant (R01 HL145709) to O.E-A., and an American Heart Association grant (17GRNT33460130) to O.E.-A. **Author contributions:** The original draft of the manuscript was written by J.K.L., and J.K.L and M.V.G. contributed to writing via review and editing. The project was conceptualized by J.K.L., M.V.G., O.D.A., E.R.B., and O.E.-A., with inputs from all authors. The investigation was carried out by J.K.L., M.V.G., O.D.A., J.D.H., D.K., and E.R.B. Methodology was done by J.K.L., M.V.G., O.D.A., D.K., E.R.B., and O.E.-A., and J.K.L., M.V.G., O.D.A., E.R.B., and O.E.-A. participated in validation. Supervision was done by J.K.L. and O.E.-A., and J.K.L. and M.V.G. contributed to formal analysis. Project administration was done by E.R.B., M.V.G., and O.E.-A. Visualization was carried out by J.K.L., M.V.G., and D.K. O.E.-A. provided resources and funding acquisition. **Competing interests:** The authors declare that they have no competing interests. **Data and materials availability:** All data needed to evaluate the conclusions in the paper are present in the paper and/or the Supplementary Materials.

Submitted 9 March 2024
Accepted 27 November 2024
Published 3 January 2025
10.1126/sciadv.adp1461